Melanoma

Test	Source	Results		P-Value
			%	
BRAF	Metastasis	Pos	50	0.023
N=333	N=294	Neg	50	
	Primary	Pos	30.7	
	N=39	Neg	69.2	
Kit	Metastasis	Pos	5.2	0.265
N=230	N=191	Neg	94.7	
	Primary	Pos	10.2	
	N=39	Neg	89.7	
KRAS	Metastasis	Pos	10.5	1.00
N=22	N=19	Neg	89.4	
	Primary	Pos	0	
	N=3	Neg	100	
NRAS	Metastasis	Pos	21.7	0.592
N=264	N=225	Neg	78.2	
	Primary	Pos	25.6	
	N=39	Neg	74.3	
PIK3CA	Metastasis	Pos	3.7	1.000
N=30	N=27	Neg	96.3	
	Primary	Pos	0	
	N=3	Neg	100	

Colorectal Adenocarcinoma

Test	Source	Result		P-Value
			%	
BRAF	Metastasis	Pos	5.8	0.116
N=564	N=137	Neg	94.1	
	Primary	Pos	10.3	
	N=427	Neg	89.7	
KIT	Metastasis	Pos	7.6	1.000
N=35	N=13	Neg	92.3	
	Primary	Pos	4.5	
	N=22	Neg	95.4	
KRAS	Metastasis	Pos	41.0	0.931
N=590	N=151	Neg	58.9	
	Primary	Pos	41.4	
	N=439	Neg	58.5	
NRAS	Metastasis	Pos	25	0.048
N=31	N=12	Neg	75	
	Primary	Pos	0	
	N=19	Neg	100	
PIK3CA	Metastasis	Pos	22.5	0.350
N=141	N=40	Neg	77.5	
	Primary	Pos	15.8	
	N=101	Neg	84.1	

Conclusions: BRAF mutation was more seen in a metastatic site rather than primary in melanoma (p=0.023). In colorectal adenocarcinoma, NRAS mutation was more likely persent in metastatic site than primary (p=0.048). We did not find association with examined site in other analyzed mutations (KRAS, KIT, PIK3CA). These results suggest importance of consideration of disease site when analyzing mutational status. Probability of co-mutations in different pathways has significance for decisions regarding therapy.

1953 Aurora Kinase Inhibitors as a Novel Targeted Drug Therapy for Bladder Cancer

N Zhou, K Singh, A Almasan, DE Hansel. Cleveland Clinic, Cleveland, OH.

Background: Conventional chemotherapy for invasive bladder cancer has limited efficacy and is generally associated with poor patient prognoses. This study aims to evaluate the potential of targeting the aurora kinases, a family of mitotic regulators, with pharmacologic inhibitors as a novel treatment for bladder cancer.

Design: Expression of genes associated with the mitotic spindle checkpoint, including the aurora kinases A and B, in clinical tissue samples of urothelial and squamous cell carcinomas was evaluated by RNA microarray and reverse-transcriptase PCR. Urothelial carcinoma cell lines UM-UC-3 and T24 were treated with the nonspecific aurora kinase inhibitor ZM447439 and the aurora kinase A inhibitor MLN8237, either alone or in combination with gemcitabine or paclitaxel. Effects of drug treatments were evaluated by flow cytometry with propidium iodide staining, immunofluorescence microscopy, MTS proliferation assay, and TUNEL labeling.

Results: RNA microarray analysis comparing human tissue specimens of urothelial (N=8) and squamous cell carcinomas (N=9) of the bladder to normal urothelium (N=10) identified overexpression of 13 gene transcripts related to the mitotic spindle checkpoint, including aurora kinases A and B, in the cancer specimens. Upregulation of these genes was validated by RT-PCR on a separate set of clinical samples (N=4 for each group). Next, we evaluated the impact of aurora kinase inhibitors on the bladder cancer cell lines in vitro. ZM447439 and MLN8237 treatment of UM-UC-3 and T24 cell lines at concentrations of 10 nM to 1 μM induced G2/M cell cycle arrest and aneuploidy (>4N DNA content) in a dose dependent manner. Immunofluorescence microscopy revealed abnormal mitotic figures with multipolar spindle apparatuses in treated cells. Both cell lines also exhibited cell death by positive TUNEL staining 48 hours after treatment with either inhibitor. Simultaneous treatment of T24 cells with MLN8237 and paclitaxel and subsequent MTS proliferation assay revealed an antagonistic interaction between paclitaxel and MLN8237, whereas simultaneous treatment with MLN8237 and gemcitabine resulted in an additive effect.

Conclusions: Several mitotic spindle checkpoint proteins, including the aurora kinases, are overexpressed in bladder cancer. Our data indicate that aurora kinase inhibitors have significant potential as a novel therapy for bladder cancer, as they induce abnormal mitosis, cell cycle arrest, and eventual death of bladder cancer cells in vitro.

Pediatrics

1954 Employment of the ADAMTS13 Assay Improved the Accuracy and Efficiency of the Diagnosis and Treatment of Suspected Acquired Thrombotic Thrombocytopenic Purpura

BD Barrows, J Teruya. Baylor College of Medicine, Houston, TX.

Background: Acquired thrombotic thrombocytopenic purpura (A-TTP) is a significant cause of microthrombotic hemolytic anemia requiring rapid diagnosis and treatment in pediatric patients. A-TTP is generally due to a circulating inhibitor of ADAMTS13 (a disintegrin and metalloproteinase with a thrombospondin type 1 motif, member 13). ADAMTS13 is responsible for the degradation of unusually large von Willebrand factor (ULVWF) multimers. Without ADAMTS13, the ULVWF multimers can indiscriminately attach to platelets precipitating microthrombosis. The primary treatment for A-TTP is therapeutic plasma exchange (TPE), which removes both the ULVWF multimers and ADAMTS13 inhibitor while replenishing ADAMTS13 via plasma infusion. TPE is an expensive and invasive procedure necessitating thoughtful reservation concerning its use as an emergent treatment modality. The ADAMTS13 activity assay has become a reliable screening method in suspected cases of A-TTP. Many hospital labs do not perform the ADAMTS13 assay, requiring sample analysis at an outside lab, delaying diagnostic confirmation by days. Therefore, most cases highly suspicious for A-TTP must be started on TPE before diagnostic confirmation.

Design: In order to determine the diagnostic value of the ADAMTS 13 assay in detecting true cases of A-TTP and directing the efficient use of TPE, a retrospective analysis was performed including ADAMTS 13 activity results collected at our Children's Hospital during 2007–2011. These data were correlated with the use of TPE as a treatment for cases highly suspicious for A-TTP and evaluated for unnecessary patient morbidity and financial cost. TPE cost was calculated to be $4,000 per procedure using fresh frozen plasma as replacement fluid three times (~$2,000) plus patient preparation and machine operating costs (~$2000).

Results: Since implementation of the ADAMTS13 assay, 95% of suspected A-TTP cases were ruled out. This prevented unnecessary patient morbidity in addition to the financial burden of TPE.

ADAMTS13 and TPE

ADAMTS 13 Activity	Number of patients	TTP confirmed	TTP ruled out	TPE prevented	Potential treatment costs avoided
<20%	12	9	3	3	$36,000
21-64%	66	0	66	66	$792,000
>64%	78	0	78	78	$936,000
Total	156	9	147	147	1,764,000

Conclusions: Both the patient and hospital would benefit from implementation of the ADAMTS13 activity assay as a point of care lab study. The patient would avoid risks and discomfort of TPE treatment while the hospital would avoid the financial burden of TPE if it is not indicated.

1955 DAX-1 and ap2 beta Are Liable Markers of Translocation Positive Alveolar Rhabdomyosarcoma (ARMS)

B Di Venosa, A Rosolen, A Zin, E Lalli, V Guzzardo, R Alaggio. Padua University, Padua, Italy; CNRS UMR, Valbonne, France.

Background: ARMS are characterized by fusions of *FOXO1* gene on chromosome 13 with *PAX3* gene on chromosome 2 or *PAX7* gene on chromosome 1 in 80% of case. Translocation positive ARMS have a distinctive biological signature on expression array. Among other genes ap2 beta and DAX-1 have been found to be over-expressed in translocation positive ARMS and a strong and diffuse nuclear immunostaining for ap2 beta appears to be predictive of presence of translocation.

Design: We studied a series of 45 ARMS (37 classic and 8 with areas of embryonal rhabdomyosarcoma-ERMS) and 25 ERMS to test the role of ap2 beta and DAX- 1 expression in predicting molecular status of ARMS.Immunostains for desmin, myogenin, ap2 beta and DAX-1 were performed. Ap2 beta and DAX-1 were considered positive when a strong and diffuse nuclear staining was found in the majority of cells.

Results: All tumors were desmin and myogenin positive, with staining for myogenin in more than 50% of cells in 78% of ARMS and 20% of ERMS respectively. Ap2 beta and DAX-1 pattern of expression are summarized in Table 1.

Ap2 beta and DAX-1 pattern

Diagnosis (70 cases)	Ap2beta+/ DAX1+	Ap2beta+/ DAX-1-	Ap2beta-/ DAX-1+	Ap2beta-/ DAX-1-
ARMS t+ (32)	25	2	3	2
Arms t- (5)	0	1	3	1
ERMS (25)	1	0	5	19
MIXED (ARMS+ERMS, t-) (8)	2	0	4	2

Legend: t+: translocation positive, t-: translocation negative.

Translocation positive ARMS show a characteristic ap2beta+ and DAX-1 + staining in 78% of cases, while 76% of classic ERMS are negative for both. Ap2 beta alone was positive in 2.6% of rhabdomyosarcomas lacking translocation whereas DAX-1 alone was positive in 31.5%, by contrary 9% and 6% of translocation positive ARMS were positive only for DAX-1 or Ap2beta respectively.Mixed ARMS and ARMS t- share the same phenotype as ERMS but have a higher frequency of DAX-1 expression (20% vs 53%).

Conclusions: Compared to Ap2 beta, DAX-1 is less specific but highly sensitive. Our results suggest that the combined use of ap2 beta and DAX-1 might be helpful in identifying classic ARMS with translocation.

1956 An Investigation of miRNAs in the Pathogenesis of Pediatric/Wild-Type Gastrointestinal Stromal Tumor

L Kelly, S Kim, K Bryan, M Debiec-Rychter, MJ O'Sullivan. Our Lady's Children's Hospital, Crumlin, Dublin 12, Ireland.

Background: Gastrointestinal stromal tumour [GIST] is characterized by activating mutations of tyrosine kinase III receptors KIT/PDGFRA, or rarely BRAF, yet a wild-type [WT] form, commonest in childhood, shows similar downstream KIT signalling but without activating TK mutation. The wild-type form is poorly responsive to targeted therapy with tyrosine kinase inhibitors such as imatinib. Genomic losses at 14q, 22q, 1p and 9p occur in adult but not pediatric GIST, which shows no consistent copy number alterations. These findings prompted our investigation of epigenetic mechanisms including miRNAs to explain cell biological dysregulation in wild-type/pediatric GIST.

Design: DNA and RNA were extracted from 45 adult and 29 pediatric GISTs. KIT exons 9, 11, 13, 17 and PDGFRA exons 12, 14, 18 were amplified from DNA, the products examined by high resolution melt analysis and those with aberrant curves sequenced. RNA applied to TaqMan Low Density Arrays (TLDAs) for miRNA profiling, examined 667 miRNAs per sample. Validation was by individual TaqMan assays. Hierarchical clustering was performed using Spearman's rank correlation and Ward's linkage. The methylation status of the 14q32 region was analyzed by allele-specific, methylation-sensitive PCR of bisulfite-converted DNA.

Results: Unsupervised hierarchical clustering clearly separated adult and pediatric cases. The adult group could be further split by differential expression of 47 miRNAs located on 14q32, due to differential allelic methylation.

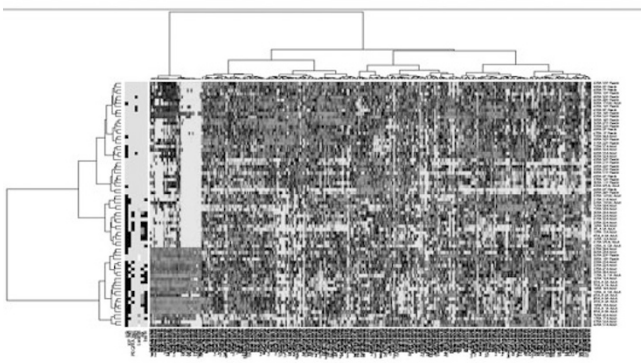

Differential miRNA expression between wild-type/pediatric and mutant GISTs revealed numerous miRNAs >5-fold differentially expressed and of statistical significance ($p<0.05$). Potential interactions between diametrically expressed miRNA and mRNA revealed significantly more interactions than expected, particularly for IGF1R.

Conclusions: This work has produced unprecedented distinct miRNA profiles for adult and pediatric GISTs. Adult GISTs are further split by high expression of a miRNA cluster on 14q32, *not* explained by 14q loss, but by differential allelic methylation. miRNA/mRNA interaction analysis reveals several significant interactions between miRNAs and genes important in WT GIST, which we are currently investigating.

1957 Confocal Microscopy Image Analysis of Pancreatic ß-Cells K^{ATP} Channel Proteins in Congenital Hyperinsulinism (CHI)

SM Lovisolo, AL Garippo, F Guedes, MC Zerbini. University of Sao Paulo Medical School, Sao Paulo, Brazil; HU-USP, Sao Paulo, Brazil; USP, Sao Paulo, Brazil.

Background: CHI is a life-threatening disorder of glucose metabolism of neonates characterized by serum insulin levels unresponsive to blood glucose concentrations. Pancreatic ß-cells regulates insulin secretion through ATP sensitive potassium channels (K^{ATP}channel) formed by sulfonylurea receptor 1 (SUR1) and potassium inward rectifying 6.2 (Kir 6.2) proteins. The ß-cell K^{ATP}channel dependent CHI is classically associated with loss-of-function mutations of these subunits genes. In a previous study [1], no mutations in the Kir6.2 gene and in the 33-37 exons *hot spot* region of the SUR1 gene were identified in these patients. The aim of this study is to investigate if these subunits were present in the ß-cells of CHI patients.

Design: Pancreatic surgical paraffin tissue from 7 neonates (3F/4M, 4-13 mo) with CHI and 8 autopsy pancreatic control tissue (5F/3M, 4-11 mo) were included in the study. Confocal microscopy double-staining immunofluorescence (insulin/SUR1 and insulin/Kir6.2) was performed in order to detect each protein specifically in the ß-cells. All sections were analyzed under a Zeiss 510 Meta confocal laser scanning microscope (63x). At least 10 different endocrine islets were captured to evaluate the expression of either Kir6.2 or SUR1 (green-488nm) and insulin (red-633nm). Co-expression of insulin/SUR1 and insulin/Kir6.2 was analysed visually (green x red→yellow) and through correlation *Pearson's coefficient* (PC) that estimates the goodness of rate association of the two fluorochromes. PC was compared among cases and controls using a nonparametric method (Mann-Whitney).

Results: Visual observation clearly revealed the presence of Kir6.2 and SUR1 in a granular cytoplasmic pattern in the ß-cells of cases and controls. Nevertheless, overlap of insulin/Kir6.2 and insulin/SUR1 seemed to be more constant and uniform in controls than in CHI cases, confirmed by the analysis through PC showing a statistically significant decrease in Kir6.2 ($P = 0.0084$) and SUR1 ($P = 0.041$) in the ß-cells of CHI patients.

Conclusions: This is the first demonstration of K^{ATP}channels subunits Kir6.2 and SUR1 in the pancreatic ß-cells of CHI patients using an *in situ* method. Our results show that both subunits were present in the ß-cells, but are under-expressed in CHI patients compared to controls, adding a new information to this rare condition with a complex pathogenesis.

[1] Lovisolo SM, Zerbini MC et al. *Ped Dev Pathol 2010;13:375-384.*

1958 Characterisation of t(10;17)(q22;p13) in Clear Cell Sarcoma of Kidney

E O'Meara, D Stack, C Lee, J Garvin, T Morris, P Argani, D Gisselsson, I Leuschner, M Gessler, N Graf, JA Fletcher, MJ O'Sullivan. Our Lady's Children's Hospital, Crumlin, Dublin, Ireland.

Background: Clear cell sarcoma of kidney [CCSK], the second commonest pediatric renal cancer is classified as unfavorable histology by the National Wilms Tumor Study group. It is diagnostically challenging, therapy-resistant and has poor outcomes. Nothing is currently known about CCSK biology. Array CGH has shown no consistent genomic aberrations. Three case reports of CCSK with balanced translocation t(10;17)(p13;q22), prompted our investigation into t(10:17), to identify the genes involved and establish translocation incidence.

Design: 51 CCSKs were sourced from Europe and North America, touch imprints for fluorescence in-situ hybridisation [FISH] made and RNA extracted. The breakpoints on chromosomes 10 and 17 were identified in the index case with t(10;17)(q22;p13), using fluorescently labelled BACs. RT-PCR with primers specific for candidate genes within the breakpoint regions was carried out to identify the fusion transcript in the index case and the product sequenced. The 50 CCSKs were screened by FISH and RT-PCR for evidence of the translocation/transcript.

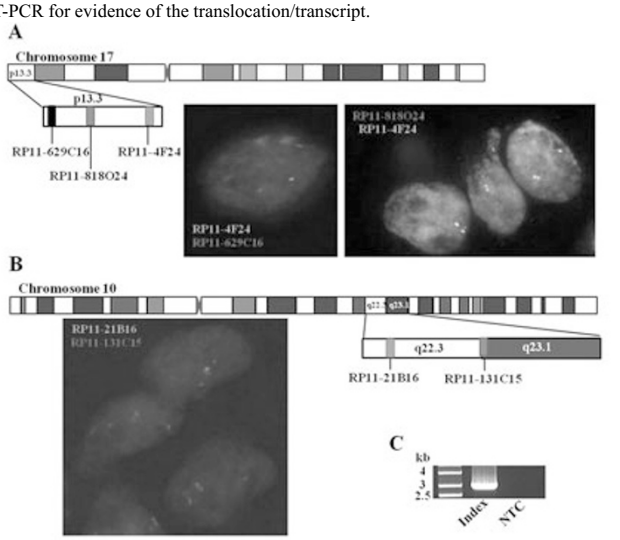

Results: t(10:17)(q22;p13) in CCSK involves YWHAE on chromosome 17 and members of the FAM22 gene family on chromosome 10. Exons 1-5 of YWHAE are fused in-frame to exons 2-7 of FAM22 genes. The YWHAE-FAM22 fusion transcript was identified in 7 of 51 CCSK cases, 12% of the total cases tested. Clinico-morphological correlates of translocation status were investigated and significant differences in tumor stage and cellularity noted between transcript-positive and transcript-negative cases.

Conclusions: Identification of the genes involved in CCSK-associated t(10:17) represents the first step in understanding CCSKmolecular genetics. Although the proportion of cases with the translocation is relatively low [12%], it is possible that the involved genes are dysregulated by alternative means in transcript-negative cases. There was a significant difference in stage of transcript-positive versus -negative cases with no transcript-positive case presenting with stage I disease, despite this representing 31% of cases. No significant differences in outcome were detectable between transcript-positive and transcript-negative cases. We are now studying the cell biological effects of expressing this transcript.